Synthesis of the 13-Vertex Rhodacarborane Anion [4-(1,2:5,6-η-cod)-*closo*-4,1,6-$RhC_2B_{10}H_{12}$]$^-$ and Its Reactions with Electrophiles

Bruce E. Hodson, Thomas D. McGrath, and F. Gordon A. Stone*

Department of Chemistry & Biochemistry, Baylor University, Waco, Texas 76798-7348

Received November 19, 2004

Reduction of *closo*-1,2-$C_2B_{10}H_{12}$, with sodium naphthalide in THF (THF = tetrahydrofuran), followed by addition of $[Rh_2(\mu\text{-}Cl)_2(cod)_2]$ (cod = 1,2:5,6-η-cyclooctadiene) and $[N(PPh_3)_2]Cl$, affords the monoanionic 13-vertex rhodacarborane $[N(PPh_3)_2][4\text{-}(cod)\text{-}closo\text{-}4,1,6\text{-}RhC_2B_{10}H_{12}]$ (**2**). Treatment of compound **2** with sources of the cations $\{Cu(PPh_3)\}^+$, $\{Rh(PPh_3)_2\}^+$, $\{Rh(cod)\}^+$, and $\{RuCl(PPh_3)_2\}^+$ yields, respectively, the neutral bimetallic species [4-(cod)-3,4,7-$\{Cu(PPh_3)\}$-3,7-(μ-H)$_2$-*closo*-4,1,6-$RhC_2B_{10}H_{10}$], [4-(cod)-3,8-$\{Rh(PPh_3)_2\}$-3,8-(μ-H)$_2$-*closo*-4,1,6-$RhC_2B_{10}H_{10}$], [4-(cod)-3,8-$\{Rh(cod)\}$-3,8-(μ-H)$_2$-*closo*-4,1,6-$RhC_2B_{10}H_{10}$], and [4-(cod)-3,7,8-$\{RuCl(PPh_3)_2\}$-3,7,8-(μ-H)$_3$-*closo*-4,1,6-$RhC_2B_{10}H_9$], of which only the copper derivative has a metal−metal bond. In addition, the reaction of **2** with CF_3SO_3H results in protonation of the cyclooctadiene ligand with concomitant oxidation of the rhodium center, yielding the ostensibly 16-electron Rh^{III} compound [4-(1−3-η^3-C_8H_{13})-*closo*-4,1,6-$RhC_2B_{10}H_{12}$], which is stabilized by a C−H···Rh agostic interaction. Alternatively, treatment of **2** with hydride-abstracting reagents in the presence of THF results in substitution at a cage BH vertex, forming the zwitterionic complex [4-(cod)-7-$\{O(CH_2)_4\}$-*closo*-4,1,6-$RhC_2B_{10}H_{11}$].

Introduction

Extensive studies with anionic icosahedral 12-vertex $\{MC_2B_9\}$ systems have revealed the ability of the metallacarborane cage to act as a "nonspectator" ligand with respect to attacking electrophiles.[1] The hydridic nature of the boron-bound cage hydrogen atoms allows for the formation of B−H⇀M′ agostic-type interactions or for direct substitution at a boron vertex by a donor ligand in the presence of a suitable hydride-abstracting agent.

Among {*closo*-RhC_2B_9} systems, several compounds exist in which the rhodium vertex carries an *exo*-polyhedral cod ligand.[2] Treatment of the compound $[N(PPh_3)_2][1,2\text{-}Me_2\text{-}3\text{-}(cod)\text{-}closo\text{-}3,1,2\text{-}RhC_2B_9H_9]$ (**1a**)[2a] (Chart 1) with a mixture of $[CuCl(PPh_3)]_4$ and $Tl[BF_4]$ in CH_2Cl_2 affords the neutral bimetallic species [1,2-Me_2-3-(cod)-3,8-$\{Cu(PPh_3)\}$-8-(μ-H)-*closo*-3,1,2-$RhC_2B_9H_8$], in which an Rh−Cu bond is supported by a B−H⇀Cu agostic-type interaction from the carborane cage unit.[2c] Interestingly, **1a** and the related salt $[NEt_4][1,2\text{-}Me_2\text{-}3\text{-}(cod)\text{-}closo\text{-}3,1,2\text{-}RhC_2B_9H_9]$ (**1b**) undergo reactions with CF_3CO_2H[2a] and $[Ph_3C][BF_4]$,[2d] respectively, to either add or abstract a proton from the cod ligand. The rhodacarborane cage remains unaffected, except for a two-electron oxidation of the rhodium center.

The established route for the synthesis of 13-vertex metallacarboranes involves the reduction of *closo*-1,2- or -1,7-$C_2B_{10}H_{12}$ to produce [*nido*-7,9-$C_2B_{10}H_{12}]^{2-}$, followed by the coordination of a metal atom to the six-atom open face of the *nido* carborane.[3] Using this methodology, a number of *closo*-$\{MC_2B_{10}\}$ (M = transition metal) systems having docosahedral architectures have been prepared.[3,4] However, except for the polyhedral expansion of a 13-vertex $\{MC_2B_{10}\}$ cage system to form a 14-vertex $\{M_2C_2B_{10}\}$ architecture,[5] the reactivity of these compounds has received little attention.

Chart 1

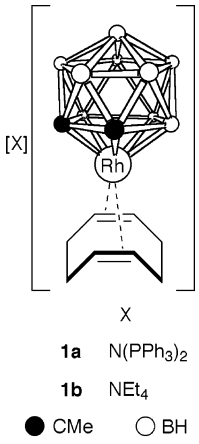

(1) Jelliss, P. A.; Stone, F. G. A. *J. Organomet. Chem.* **1995**, *500*, 307.

(2) (a) Speckman, D. M.; Knobler, C. B.; Hawthorne, M. F. *Organometallics* **1985**, *4*, 426. (b) Pilotti, M. U.; Stone, F. G. A.; Topaloğlu, I. *J. Chem. Soc., Dalton Trans.* **1991**, 1621. (c) Jeffery, J. C.; Stone, F. G. A.; Topaloğlu, I. *J. Organomet. Chem.* **1993**, *451*, 205. (d) Jeffery, J. C.; Stone, F. G. A.; Topaloğlu, I. *Polyhedron* **1993**, *12*, 319. (e) Hodson, B. E.; Ellis, D.; Rosair, G. M.; Welch, A. J. *Angew. Chem., Int. Ed.* **2001**, *40*, 715.

(3) (a) Dunks, G. B.; McKown, M. M.; Hawthorne, M. F. *J. Am. Chem. Soc.* **1971**, *93*, 2541. (b) Callahan, K. P.; Hawthorne, M. F. *Adv. Organomet. Chem.* **1976**, *14*, 145.

(4) Examples include: (a) Dustin, D. F.; Dunks, G. B.; Hawthorne, M. F. *J. Am. Chem. Soc.* **1973**, *95*, 1109. (b) Carr, N.; Mullica, D. F.; Sappenfield, E. L.; Stone, F. G. A.; Went, M. J. *Organometallics* **1993**, *12*, 4350. (c) Mullica, D. F.; Sappenfield, E. L.; Stone, F. G. A.; Woollam, S. F. *Can. J. Chem.* **1995**, *73*, 909. (d) Burke, A.; McIntosh, R.; Ellis, D.; Rosair, G. M.; Welch, A. J. *Collect. Czech. Chem. Commun.* **2002**, *67*, 991. (e) Laguna, M. A.; Ellis, D.; Rosair, G. M.; Welch, A. J. *Inorg. Chim. Acta* **2003**, *347*, 161.

10.1021/om049102e CCC: $30.25
Publication on Web 02/25/2005

Table 1. Analytical and Physical Data[a]

cmpd	color	yield (%)	anal.[b] (%) C	anal.[b] (%) H
$[N(PPh_3)_2][4\text{-}(cod)\text{-}closo\text{-}4,1,6\text{-}RhC_2B_{10}H_{12}]$ (**2**)	brown	56	62.8 (63.2)[c]	6.2 (6.2)
$[4\text{-}(cod)\text{-}3,4,7\text{-}\{Cu(PPh_3)\}\text{-}3,7\text{-}(\mu\text{-}H)_2\text{-}closo\text{-}4,1,6\text{-}RhC_2B_{10}H_{10}]$ (**3**)	yellow	48	49.6 (49.4)	5.8 (5.8)
$[4\text{-}(cod)\text{-}3,8\text{-}\{Rh(PPh_3)_2\}\text{-}3,8\text{-}(\mu\text{-}H)_2\text{-}closo\text{-}4,1,6\text{-}RhC_2B_{10}H_{10}]$ (**4**)	orange	61	56.2 (56.2)	5.5 (5.5)
$[4\text{-}(cod)\text{-}3,8\text{-}\{Rh(cod)\}\text{-}3,8\text{-}(\mu\text{-}H)_2\text{-}closo\text{-}4,1,6\text{-}RhC_2B_{10}H_{10}]$ (**5**)	yellow	49	43.2 (43.3)[d]	7.6 (7.6)
$[4\text{-}(cod)\text{-}3,7,8\text{-}\{RuCl(PPh_3)_2\}\text{-}3,7,8\text{-}(\mu\text{-}H)_3\text{-}closo\text{-}4,1,6\text{-}RhC_2B_{10}H_9]$ (**6**)	red	35	55.8 (55.9)[e]	6.1 (6.1)
$[4\text{-}(1\text{-}3\text{-}\eta^3\text{-}C_8H_{13})\text{-}closo\text{-}4,1,6\text{-}RhC_2B_{10}H_{12}]$ (**7**)	orange	76	33.7 (33.7)	7.1 (7.1)
$[4\text{-}(cod)\text{-}7\text{-}\{O(CH_2)_4\}\text{-}closo\text{-}4,1,6\text{-}RhC_2B_{10}H_{11}]$ (**8**)	yellow	81	39.3 (39.4)	7.3 (7.3)

[a] IR spectra (CH_2Cl_2) all show a broad, medium-intensity band at ca. 2550 cm^{-1} due to B−H absorptions. [b] Calculated values are given in parentheses. In addition, for **2**: N 1.5 (1.5). [c] Cocrystallized with 0.5 molar equiv of C_7H_8. [d] Cocrystallized with 1.0 molar equiv of C_5H_{12}. [e] Cocrystallized with 2.0 molar equiv of THF.

Chart 2

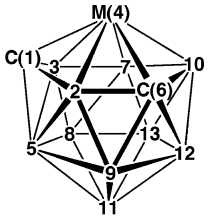

We have recently described reactions between cationic metal−ligand fragments and the anion of $[NEt_4][4\text{-}(\eta^3\text{-}C_3H_5)\text{-}closo\text{-}4,1,6\text{-}NiC_2B_{10}H_{12}]$[6] (vertexes are numbered as in Chart 2). These experiments afforded further examples of the rare class of 13-vertex metallacarboranes in which a metal fragment is bound *exo*-polyhedrally to an $\{MC_2B_{10}\}$ cage via B−H⇀M agostic-type interactions.[1] In view of the diverse chemistry of the 12-vertex $\{(cod)RhC_2B_9\}$ systems,[2] and in an effort to further investigate the reactivity of monoanionic 13-vertex metallacarboranes toward electrophiles, we now report the synthesis, characterization, and reactions of the 13-vertex rhodacarborane $[N(PPh_3)_2][4\text{-}(cod)\text{-}closo\text{-}4,1,6\text{-}RhC_2B_{10}H_{12}]$ (**2**).

Results and Discussion

The two-electron reduction of *closo*-1,2-$C_2B_{10}H_{12}$ using sodium metal in the presence of naphthalene, followed by addition of $[Rh_2(\mu\text{-}Cl)_2(cod)_2]$ and then $[N(PPh_3)_2]Cl$, results in the formation of the 13-vertex rhodacarborane $[N(PPh_3)_2][4\text{-}(cod)\text{-}closo\text{-}4,1,6\text{-}RhC_2B_{10}H_{12}]$ (**2**) (Chart 3). Compound **2** is characterized by the data in Tables 1−3. Six resonances in a 1:2:1:3(2+1 coincidence):1:2 intensity ratio are seen in its $^{11}B\{^1H\}$ NMR spectrum, indicating that the molecule retains pseudo-C_s symmetry in solution.[4a] A ^1H NMR study revealed characteristic signals due to the cod ligand with a sharp singlet of relative intensity 4 due to the =CH groups at δ 4.06 and two multiplet resonances at δ 2.39 and 2.30 due to the remaining eight CH_2 protons. Likewise, the $^{13}C\{^1H\}$ NMR spectrum of **2** displayed a doublet (J(RhC) = 11 Hz) due to the methine groups of the cod ligand at δ 77.3, with the methylene carbon atoms of the ring appearing as a single peak at δ 32.3.

An X-ray crystallographic study of **2** established the molecular structure shown in Figure 1. The rhodium atom is coordinated in a hexahapto manner by the six-atom CBCBBB open face of the carborane cage. The cod ligand is orientated such that the centroids of the ligating ene functionalities lie within a plane running through B(2), B(7), and B(11). This orientation has some precedent in 12-vertex $\{closo\text{-}2,1,7\text{-}MC_2B_9\}$ systems,[7] although it may also be influenced by crystal packing forces.

Chart 3

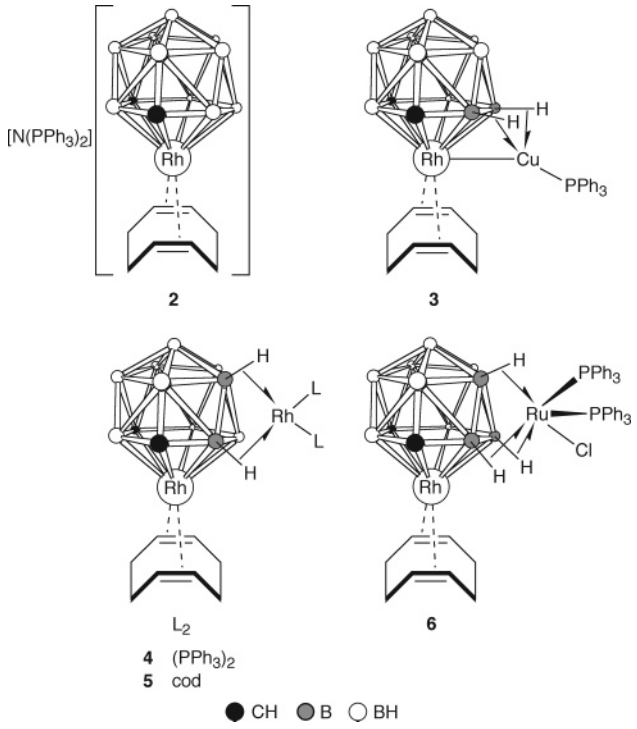

Treatment of **2** with a mixture of $[CuCl(PPh_3)]_4$ and $Tl[PF_6]$ in CH_2Cl_2 yields the neutral bimetallic species $[4\text{-}(cod)\text{-}3,4,7\text{-}\{Cu(PPh_3)\}\text{-}3,7\text{-}(\mu\text{-}H)_2\text{-}closo\text{-}4,1,6\text{-}RhC_2B_{10}H_{10}]$ (**3**). The $^{11}B\{^1H\}$ NMR spectrum of **3** (Table 3) is rather broad and uninformative, consisting of four convoluted peaks in intensity ratio 1:2:4:3 and perhaps suggesting an asymmetric cage system. A ^1H NMR study of **3** reveals a broad singlet peak at δ 4.21 corresponding to the four methine group protons of the cod ligand, with the remaining eight protons appearing as two multiplet signals, both of relative intensity 4, at δ 2.40 and 2.18. The phenyl groups of the *exo*-$\{Cu(PPh_3)\}$ fragment give rise to a complex set of multiplet resonances in the region δ 7.78−7.52, the phosphorus atom of this group appearing as a broad peak at δ 5.7 in the $^{31}P\{^1H\}$ NMR spectrum (Table 3).

(5) For example: Evans, W. J.; Hawthorne, M. F. *J. Chem. Soc., Chem. Commun.* **1974**, 38.
(6) Hodson, B. E.; McGrath, T. D.; Stone, F. G. A. *Dalton Trans.* **2004**, 2570.

Table 2. ^{1}H and ^{13}C NMR Data[a]

cmpd	^{1}H/δ [b]	^{13}C/δ [c]
2	7.95−7.54 (m, 30H, Ph), 4.06 (br s, 4H, =CH), 3.47 (br s, 2H, cage CH), 2.39 (m, 4H, CH_2), 2.30 (m, 4H, CH_2)	131.5−126.4 (Ph), 77.3 (d, J(RhC) = 11, =CH), 59.8 (cage CH), 32.3 (CH_2)
3	7.78−7.52 (m, 15H, Ph), 4.21 (br s, 4H, =CH), 3.54 (br s, 2H, cage CH), 2.40 (m, 4H, CH_2), 2.18 (m, 4H, CH_2)	134.0−129.3 (Ph), 83.0 (d, J(RhC) = 9, =CH), 61.6 (cage CH), 32.7 (CH_2)
4	7.53−7.17 (m, 30H, Ph), 4.01 (br s, 4H, =CH), 3.25 (br s, 2H, cage CH), 2.16 (s, 8H, CH_2)	135.3−125.8 (Ph), 80.4 (d, J(RhC) = 10, =CH), 58.1 (cage CH), 31.9 (CH_2)
5[d]	5.18 (br m, 4H, *exo* =CH), 4.19 (s, 4H, *endo* =CH), 3.57 (br s, 2H, cage CH), 2.43 (br m, 4H + 4H, *exo*/*endo* CH_2), 2.30 (q, J(HH) = 8, 4H, *exo* CH_2), 2.04 (q, J(HH) = 9, 4H, *endo* CH_2)	82.4 (d, J(RhC) = 13, *exo* =CH), 81.8 (d, J(RhC) = 10, *endo* =CH), 61.3 (cage CH), 32.2 (*endo* CH_2), 31.0 (*exo* CH_2)
6	7.43−7.10 (m, 30H, Ph), 4.76 (br s, 1H, cage CH), 4.56 (br s, 2H, =CH), 4.34 (br s, 2H, =CH), ca. 2.5 (br sh, 1H, cage CH), 2.46 (br m, 4H, CH_2), 2.30 (br m, 4H, CH_2), ca. −3.2 (vbr, 1H, B−H⇀Ru), ca. −5.0 (br, 1H, B−H⇀Ru), ca. −15.4 (br, 1H, B−H⇀Ru)	135.1−127.0 (Ph), 82.4 (d, J(RhC) = 11, =CH), 78.6 (br d, J(RhC) ∼ 8, =CH), 64.4 (br, cage CH), 57.4 (br, cage CH), 32.3 (CH_2), 31.4 (CH_2)
7[e]	5.63 (br, 2H, H^1 and H^3), 4.43 (td, J(HH) = 8, J(RhH) ∼ 1, 1H, H^2), 2.47 (br, 2H, H^4 and H^8), 1.76 (br, 2H, H^5 and H^7), 1.58 (br, 2H, H^5 and H^7), 1.49 (m, 1H, H^6), 1.35 (m, 1H, H^6)	99.4 (d, J(RhC) = 6, C^2), ca. 93 (v br, C^1 and C^3), 28.6 (v br, C^4, C^5, C^7, and C^8), 23.0 (C^6)
	At 233 K: 6.00 (m, 1H, H^1), 5.39 (m, 1H, H^3), 4.54 (vt, J(HH) = J(HH) = 7,1H, H^2), 2.67 (m, 1H, H^4), 2.36 (m, 1H, H^{8b}), 1.90 (br m, 1H, H^7), 1.82 (br m, 1H, H^7), 1.69 (br m, 1H, H^5), 1.59 (m, 1H, H^5), 1.57 (m, 2H, H^4 and H^6), 1.41 (br m, 1H, H^6), −1.01 (br, 1H, H^{8a})	At 233 K: 98.4 (d, J(RhC) = 5, C^2), 93.5 (br, C^1), 78.0 (d, J(RhC) = 11, C^3), 33.6 (C^4), 29.4 (C^5), 28.1 (C^8), 26.8 (C^7), 21.7 (br, C^6)
8	4.85 (br s, 4H, OCH_2), 4.05 (br s, 4H, =CH), 3.11 (br s, 2H, cage CH), 2.42 (m, 8H, =CHCH_2), 2.32 (m, 4H, OCH_2CH_2)	81.3 (OCH_2), 80.9 (d, J(RhC) = 11, =CH), 55.3 (cage CH), 32.2 (=$CHCH_2$), 25.2 (OCH_2CH_2)

[a] Chemical shifts (δ) in ppm, coupling constants (J) in hertz; measurements in CD_2Cl_2 at ambient temperatures, except where indicated. [b] Resonances for terminal BH protons occur as broad unresolved signals in the range δ ca. −1 to +3. [c] ^{1}H-decoupled chemical shifts are positive to high frequency of $SiMe_4$. [d] For compound **5**, *exo* and *endo* refer to the cod ligand bound to the *exo*-polyhedral rhodium atom or to the rhodium vertex of the rhodacarborane cage, respectively. [e] Atoms in the $\{C_8H_{13}\}$ ligand are labeled as shown below; signals for the carborane CH units could not conclusively be assigned, while the resonances for the C−*H*···Rh protons are too broad to be seen at room temperature.

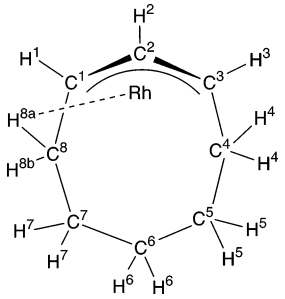

Table 3. ^{11}B and ^{31}P NMR Data[a]

cmpd	^{11}B/δ [b]	^{31}P/δ [c]
2	3.3, −3.5 (2B), −7.1, −10.9 (3B), −18.0 (2B), −22.3	
3	−3.7, −7.5 (2B), −9.2 (4B), −15.8 (3B)	5.7 (br)
4	1.2, −6.0 (2B), −7.8 (2B), −16.0 (3B), −18.6, −22.0	42.7 (d, J(RhP) = 179)
5	−6.2 (3B), −7.8 (2B), −16.4 (2B), −18.0 (2B), −20.2	
6	−5.7 (br), −7.2 (br), −12.6 (br, 3B), −19.0 (br, 4B), −24.0 (br)	55.7 (br), 43.3 (br d, J(PP) = 30)
7	11.9 (br), 6.0 (2B), 0.4 (2B), −4.1 (3B), −21.1 (2B)	
8	20.9 (B(7)), −8.1 (3B), −11.4 (2B), −13.6, −18.7 (2B), −24.1	

[a] Chemical shifts (δ) in ppm, coupling constants (J) in hertz, measurements at ambient temperatures in CD_2Cl_2. [b] ^{1}H-decoupled chemical shifts are positive to high frequency of BF_3·OEt_2 (external); resonances are of unit integral except where indicated. [c] ^{1}H-decoupled chemical shifts are positive to high frequency of 85% H_3PO_4 (external).

An X-ray crystallographic study of **3** revealed the molecular structure shown in Figure 2. The {*closo*-RhC_2B_{10}} cage system is retained, while the rhodium vertex has become involved in a metal−metal bonding interaction with the *exo*-copper atom (Rh−Cu = 2.7317(3) Å). This bond is supported by two B−H⇀Cu agostic interactions from {BH} units of the rhodacarborane cage, one being in an α (CBC*B*BB) and the other a β (CBCB*B*B) position with respect to the carbon atoms in the ligating face of the carborane (Cu···B(3) is 2.276(2) Å and Cu···B(7) is 2.129(2) Å).

Similar to the formation of **3**, treatment in CH_2Cl_2 of **2** with 1 molar equiv of sources of $\{Rh(PPh_3)_2\}^+$ or $\{Rh(cod)\}^+$ results in formation of the neutral dirhodium species [4-(cod)-3,8-$\{Rh(PPh_3)_2\}$-3,8-(μ-H)$_2$-*closo*-4,1,6-$RhC_2B_{10}H_{10}$] (**4**) and [4-(cod)-3,8-{Rh(cod)}-3,8-(μ-H)$_2$-*closo*-4,1,6-$RhC_2B_{10}H_{10}$] (**5**), respectively.

Compound **4** displays six resonances in its ^{11}B{^{1}H} NMR spectrum in the integration ratio 1:2:2:3(2+1 coincidence):1:1. This pattern suggests a time-averaged C_s symmetry in comparison to previous studies.[4a] A ^{31}P{^{1}H} NMR study of **4** reveals a doublet resonance at δ 42.7 (J(RhP) = 179 Hz), suggesting a dynamic process associated with the $\{Rh(PPh_3)_2\}^+$ fragment to be in effect that renders the two phosphorus atoms equivalent on the NMR time scale. This observation has precedence in the related compound [4-(η^3-C_3H_5)-3,8-$\{Rh(PPh_3)_2\}$-

3,8-(μ-H)$_2$-*closo*-4,1,6-$NiC_2B_{10}H_{10}$], in which the *exo* rhodium fragment was found to undergo both rotational and translational dynamic processes with respect to the cluster at ambient temperatures.[6] The phenyl groups of the PPh_3 ligands in **4** appear in the ^{1}H NMR spectrum as a set of complex multiplet peaks in the region δ = 7.53−7.17. Also observed therein are the methine group protons of the cod ligand, which appear as a broad singlet resonance at δ 4.01, with the remaining eight methylene protons seen as a singlet peak at δ 2.16.

The molecular structure of **4** derived from an X-ray diffraction study is shown in Figure 3. No apparent symmetry exists within the molecule in the solid state, lending weight to the argument that in solution the {Rh(PPh_3)$_2$} fragment is free to rotate and translate about the cage surface, leading to the observed ^{31}P{^{1}H} NMR spectrum. The *exo*-polyhedral {Rh(PPh_3)$_2$}$^+$ moiety is attached to the rhodacarborane cage via two B−H⇀Rh agostic interactions, one derived from a {BH} vertex α to a carbon atom in the ligating carborane (CBC*B*BB) face (B(3)···Rh(2) = 2.3483(18) Å) and the second from an adjacent vertex in the lower pentagonal belt (B(8)···Rh(2) = 2.3386(19) Å). A preference for this arrangement in the solid state was also observed in the related nickel compound [4-(η^3-C_3H_5)-3,8-{Rh(PPh_3)$_2$}-3,8-(μ-H)$_2$-*closo*-4,1,6-$NiC_2B_{10}H_{10}$].[6]

The ^{11}B{^{1}H} NMR spectrum of **5** is convoluted in comparison to that of **4**, containing five resonances in intensity ratio 3:2:2:2:1. The ^{1}H NMR spectrum is also complicated, but a ^{1}H−^{1}H COSY experiment allowed the assignment of peaks to the individual cod ligands. The "*endo*" cod ligand, i.e., that bound to the rhodium vertex within the metallacarborane cage, gives rise to peaks very similar to those of the corresponding ligand in **2**−**4**. Its =CH protons appear as a broad singlet peak at δ 4.19, while its CH_2 protons are observed as two multiplets at δ 2.43 and 2.04, the former of which is coincident with four of the CH_2 protons from the other, "*exo*" cod ligand. In the *exo* cod unit, the =CH groups are deshielded in comparison to those of the *endo* ligand and appear as a broad singlet resonance at δ 5.18, while four of its CH_2 protons give rise to a quartet resonance at δ 2.30, and the remaining four resonate, as mentioned, at δ 2.43. The two cod moieties are also distinguishable in the ^{13}C{^{1}H} NMR spectrum of **5**, there being doublet peaks due to the coordinated CH groups of the *endo* and *exo* ligands at δ 82.4 and 81.8, respectively.

An X-ray crystallographic study of **5** showed the molecular structure in Figure 4. The coordination of the *exo*-polyhedral rhodium fragment to the cluster surface in the solid state is essentially identical with that observed for compound **4**. It is supported by two B−H⇀Rh agostic-type interactions derived from the same respective boron vertexes as in **4**. Their geometry is similar to those in **4**, with the B(3)···Rh(2) distance being 2.349(10) Å and B(8)···Rh(2) 2.343(10) Å.

Addition of 1 molar equiv of [$RuCl_2(PPh_3)_3$] to a CH_2Cl_2 solution of **2** also affords a bimetallic complex, namely, [4-(cod)-3,7,8-{RuCl(PPh_3)$_2$}-3,7,8-(μ-H)$_3$-*closo*-4,1,6-$RhC_2B_{10}H_9$] (**6**). A number of other heteroborane cluster compounds have been reported that carry an *exo*-polyhedral {RuCl(PPh_3)$_2$}$^+$ unit, bound to the carborane surface via agostic-type B−H⇀Ru interactions, and in

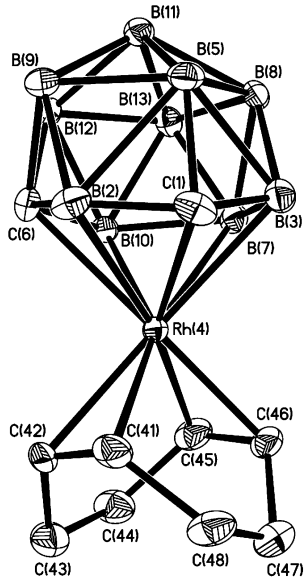

Figure 1. Structure of the anion of **2** showing the crystallographic labeling scheme. In this and in Figures 2−7 thermal ellipsoids are drawn at the 40% probability level, and for clarity only the *ipso* carbons of phenyl rings and only chemically significant hydrogen atoms are shown. Selected bond lengths (Å) and angles (deg): Rh(4)−C(1) 2.209(3), Rh(4)−B(2) 2.278(3), Rh(4)−B(3) 2.380(3), Rh(4)−C(6) 2.363(3), Rh(4)−B(7) 2.239(3), Rh(4)−B(10) 2.255(3), Rh(4)−C(41) 2.212(3), Rh(4)−C(42) 2.211(3), Rh(4)−C(45) 2.135(3), Rh(4)−C(46) 2.126(3), C(41)−C(42) 1.406(4), C(45)−C(46) 1.428(4); C(46)−Rh(4)−C(41) 80.74(10), C(45)−Rh(4)−C(41) 96.21(11), C(46)−Rh(4)−C(42) 88.78(10), C(45)−Rh(4)−C(42) 79.98(10).

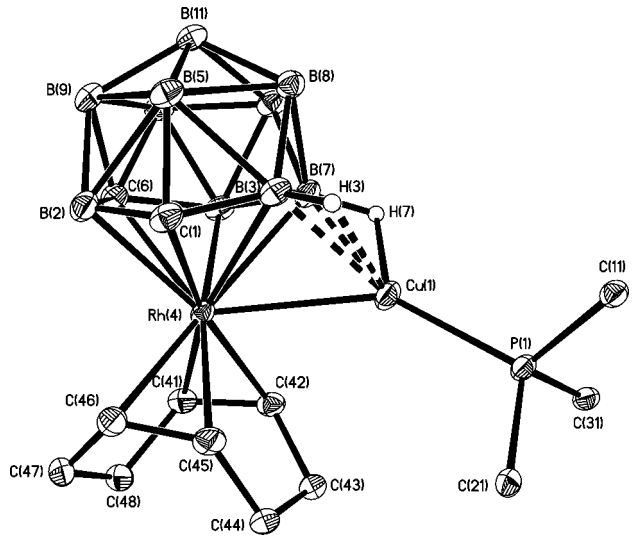

Figure 2. Structure of **3** showing the crystallographic labeling scheme. Selected bond lengths (Å) and angles (deg): Rh(4)−C(41) 2.1756(18), Rh(4)−C(42) 2.1865(17), Rh(4)−C(45) 2.1929(17), Rh(4)−C(46) 2.1784(17), Rh(4)−Cu(1) 2.7317(3), C(41)−C(42) 1.403(3), C(45)−C(46) 1.414(3), B(3)···Cu(1) 2.276(2), B(7)···Cu(1) 2.1286(19), Cu(1)−P(1) 2.1976(5); B(7)−Rh(4)−Cu(1) 48.67(5), B(3)−Rh(4)−Cu(1) 52.18(5), B(7)−Cu(1)−P(1) 155.24(6), P(1)−Cu(1)−B(3) 140.35(6), P(1)−Cu(1)−Rh(4) 146.693(15), B(3)−Cu(1)−Rh(4) 56.39(5).

which the *exo*-polyhedral metal center is not involved in a direct metal−metal bond. Variable-temperature NMR studies have shown that in some of these compounds this unit is free to rotate and translate with

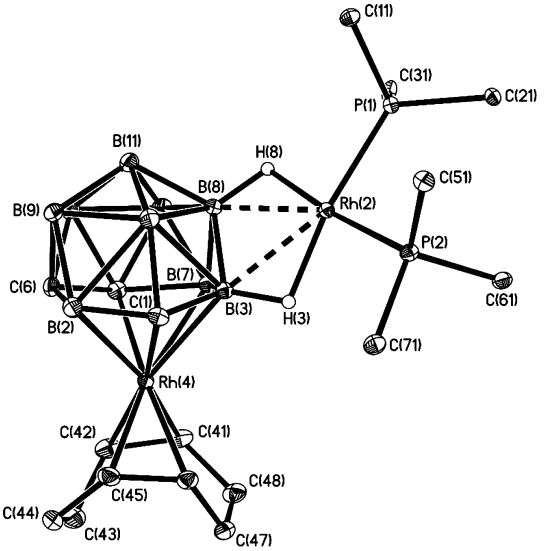

Figure 3. Structure of **4** showing the crystallographic labeling scheme. Selected bond lengths (Å) and angles (deg): Rh(4)−C(41) 2.1508(16), Rh(4)−C(42) 2.1642(18), Rh(4)−C(45) 2.1563(17), Rh(4)−C(46) 2.1714(16), C(41)−C(42) 1.403(3), C(45)−C(46) 1.399(2), B(3)···Rh(2) 2.3483(18), B(8)···Rh(2) 2.3386(19), Rh(2)−P(1) 2.2610(4), Rh(2)−P(2) 2.2425(4); C(41)−Rh(4)−C(45) 96.34(7), C(45)−Rh(4)−C(42) 79.68(7), C(41)−Rh(4)−C(46) 80.38(7), C(42)−Rh(4)−C(46) 87.57(7), P(2)−Rh(2)−P(1) 95.010(16), P(1)−Rh(2)−B(3) 153.57(5), P(2)−Rh(2)−B(3) 111.22(5), P(1)−Rh(2)−B(8) 110.27(5), P(2)−Rh(2)−B(8) 152.36(5).

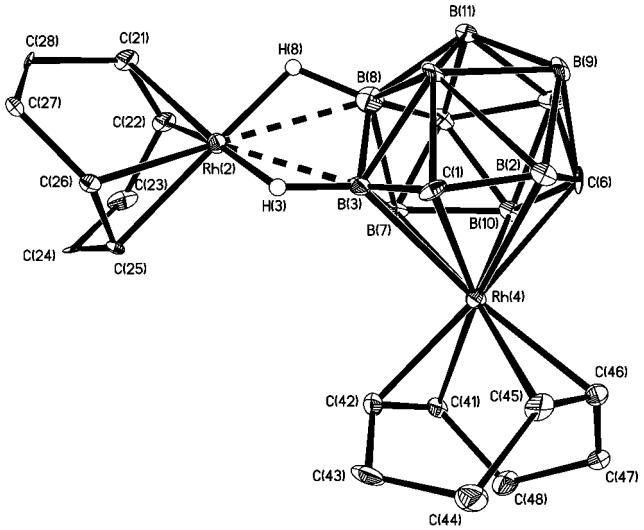

Figure 4. Structure of **5** showing the crystallographic labeling scheme. Selected bond lengths (Å) and angles (deg): Rh(4)−C(41) 2.131(7), Rh(4)−C(42) 2.122(7), Rh(4)−C(45) 2.194(7), Rh(4)−C(46) 2.162(7), C(41)−C(42) 1.437(9), C(45)−C(46) 1.406(9), B(3)···Rh(2) 2.349(10), B(8)···Rh(2) 2.343(10), Rh(2)−C(21) 2.135(7), Rh(2)−C(22) 2.138(8), Rh(2)−C(25) 2.128(7), Rh(2)−C(26) 2.119(6), C(21)−C(22) 1.388(9), C(25)−C(26) 1.393(9); C(41)−Rh(4)−C(45) 88.7(3), C(41)−Rh(4)−C(46) 79.3(3), C(42)−Rh(4)−C(45) 80.2(3), C(42)−Rh(4)−C(46) 95.8(3), C(25)−Rh(2)−C(21) 89.5(3), C(26)−Rh(2)−C(21) 82.1(3), C(25)−Rh(2)−C(22) 82.3(3), C(26)−Rh(2)−C(22) 99.0(3), C(21)−Rh(2)−B(8) 115.5(3), C(22)−Rh(2)−B(8) 107.0(3), C(25)−Rh(2)−B(8) 150.2(3), C(26)−Rh(2)−B(8) 153.4(3), C(21)−Rh(2)−B(3) 157.0(3), C(22)−Rh(2)−B(3) 141.6(3), C(25)−Rh(2)−B(3) 113.6(3), C(26)−Rh(2)−B(3) 115.2(3).

respect to the carborane surface.[8] Conversely, situations have been reported in which the Ru fragment is static on the NMR time scale and the compound exists as inseparable isomers.[6,9]

The NMR data for compound **6** (Tables 2 and 3) suggested the presence of a single, asymmetric species. Peaks in the $^{11}B\{^1H\}$ NMR spectrum were broad and convoluted, and hence rather uninformative, while the $^{31}P\{^1H\}$ NMR spectrum consisted of two broad peaks, at least one of which showed some doublet structure with a coupling constant of around 30 Hz. The latter would be typical for two inequivalent PPh_3 groups on an Ru center. Although it at first appeared in the ^1H NMR spectrum that two isomers were present, $^1H-^1H$ correlation spectroscopy confirmed that the multiple peaks for the cod ligand were due to a single moiety. The conventional ^1H NMR study showed two peaks in the region expected for the =CH units of the cod ligand at δ 4.56 and 4.34, each corresponding in intensity to two protons. In conjunction with this, two separate ^{103}Rh-coupled doublet peaks were observed in the $^{13}C\{^1H\}$ NMR spectrum at δ 82.4 and 78.6 in positions typical for these groups. Likewise, two separate unresolved multiplet peaks were observed in the ^1H NMR spectrum for the methylene groups (δ 2.46 and 2.30, each of intensity 4), along with two corresponding peaks in the $^{13}C\{^1H\}$ NMR spectrum at δ 32.3 and 31.4. The cage CH units are also seen to be inequivalent in the ^1H and $^{13}C\{^1H\}$ NMR spectra. Moreover, in the high-field region of the ^1H NMR spectrum were observed three broad resonances in the ratio 1:1:1 due to three inequivalent B−H⇀Ru agostic interactions. Of these, the two higher frequency resonances (δ ca. −3.2 and −5.0) are attributed to BH groups *trans* to PPh_3, while the more deshielded peak (δ ca. −15.4) is due to the BH *trans* to Cl. A discussion of the molecular structure at this point is beneficial in understanding the NMR data.

The structure of compound **6** derived from an X-ray diffraction study is shown in Figure 5. As is typical[6] of compounds bearing an *exo*-polyhedral $\{RuCl(PPh_3)_2\}^+$ fragment, this unit is bound to the rhodacarborane solely by B−H⇀Ru agostic-type interactions. There are three such bonds, two derived from {BH} units lying α and β (B(3) and B(7), respectively) with respect to the carbon atoms from the CBCBBB ligating face and the third from an adjacent {BH} in the upper pentagonal B_5 belt (B(8)). The weaker *trans* influence of the ruthenium-bound Cl versus PPh_3 ligands induces a shortening of the Ru···B distance *trans* to the chloride: Ru(1)···B(8) is 2.261(2) Å, whereas Ru(1)···B(3) and Ru(1)···B(7) are slightly longer at 2.324(2) and 2.465(2) Å, respectively. This arrangement is quite obviously asymmetric and presumably corresponds to the form observed in solution by NMR spectroscopy.

With the *exo*-polyhedral ruthenium fragment located over the B(3)B(7)B(8) face, the cluster lacks mirror symmetry, even with connectivity exchange between the two cage carbon atoms as discussed elsewhere.[6] Free

(7) Hodson, B. E.; McGrath, T. D.; Stone, F. G. A. *Inorg. Chem.* **2004**, *43*, 3090.
(8) Ellis, D. D.; Franken, A.; Jelliss, P. A.; Kautz, J. A.; Stone, F. G. A.; Yu, P.-Y. *J. Chem. Soc., Dalton Trans.* **2000**, 2509.
(9) Ellis, D. D.; Jelliss, P. A.; Stone, F. G. A *Organometallics* **1999**, *18*, 4982.

Chart 4

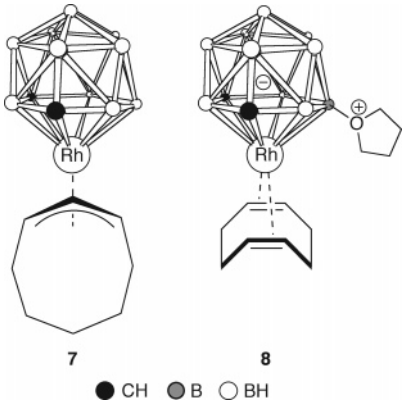

rotation of the {Rh(cod)} moiety with respect to the carborane face would only, therefore, allow the rhodium fragment time-averaged C_2 (and not C_{2v}) symmetry. Thus, for example, all four methine groups of the cod ligand are not equivalent, but the two pairs C(41)/C(45) and C(42)/C(46) (crystallographic labeling) *are* equivalent, and hence two =CH environments are seen in the ^{1}H and ^{13}C{^{1}H} NMR spectra; similar considerations would apply to the methylene groups. The presence of only three signals for B−H⁀Ru protons indicates that the {RuCl(PPh$_3$)$_2$} unit is static above the B_3 face. The situation in **6** is in marked contrast to that in the compound [4-(η^3-C_3H_5)-3,7,8-{RuCl(PPh$_3$)$_2$}-3,7,8-(μ-H)$_3$-*closo*-4,1,6-$NiC_2B_{10}H_9$],[6] in which both symmetric and asymmetric isomers exist in solution, the two differing in terms of which {BH} vertexes were involved in bridging to the Ru center. The existence of the corresponding symmetric isomer of **6** cannot be ruled out, and it may be that in the present system its concentration is too low (and its NMR resonances too broad) to permit its detection.

Previous studies[2a,d] have shown that the 12-vertex rhodacarborane anion of compounds **1** also reacts with other simple electrophiles. Thus, protonation of **1a** affords a neutral, 16-electron Rh(III) species, [1,2-Me$_2$-3-(1−3-η^3-C_8H_{13})-*closo*-3,1,2-$RhC_2B_9H_9$],[2a] whereas compound **1b** with the hydride-abstracting reagent [Ph$_3$C][BF$_4$] gives an 18-electron Rh(III) species, [1,2-Me$_2$-3-(1−3:5,6-η^5-C_8H_{11})-*closo*-3,1,2-$RhC_2B_9H_9$].[2d] It was clearly of interest, therefore, to investigate the reactivity of the closely related 13-vertex compound **2** with similar electrophilic reagents, with a view to examining its comparative reactivity.

Upon addition of CF_3SO_3H to a THF solution of **2**, the 13-vertex complex [4-(1−3-η^3-C_8H_{13})-*closo*-4,1,6-$RhC_2B_{10}H_{12}$] (**7**) (Chart 4), analogous to the product obtained by protonation of **1a**, is formed via formal protonation and two-electron reduction of the cod ligand with concomitant oxidation of the rhodium center. X-ray diffraction analysis upon crystals of **7** revealed the molecular structure shown in Figure 6. The η^3 coordination of the $\{C_8H_{13}\}^-$ ligand is clearly shown, while the rhodium atom remains η^6 coordinated by the CBCBBB face of the carborane cage. In addition to these interactions, however, there is clearly a close approach between the CH_2 unit at C(48) and the metal vertex (Rh(4)···C(48) is 2.6052(11) Å), such that one of the methylene hydrogens is close to the rhodium center (Rh(4)···H(48B) is 2.183(15) Å). This is much longer than, for example, the Rh···H separation in the B−H···Rh agostic-type interactions in compounds **4** and **5** (typically ca. 1.7 Å) but is within the reported range of conventional C−H···Rh agostic bonds (typically ca. 1.9−2.4 Å) found in the literature.[10] Nevertheless, the approach here does constitute a close contact and is significant in terms of the formal 16-electron configuration of the rhodium, as such an interaction would generate an 18-electron center. Crucially, the refined C(48)−H(48B) distance is 1.071(15) Å, somewhat longer than would be expected for a simple methylene C−H bond. In the {RhC_2B_9} analogue of **7** referred to above, there is no such short Rh···H approach (the closest is over 2.5 Å), but it is arguable that in that case the electron-donating carborane-bound methyl groups would assist in stabilizing the 16-electron metal center without recourse to any agostic interaction.

No direct supporting evidence for a C−H···Rh agostic bond is seen in NMR experiments at room temperature (see Table 2): in solution the interaction with rhodium can be envisaged as "switching" between hydrogens on C(48) and C(44) (crystallographic numbering; equivalent to C^8 and C^4 in Table 2), thereby lending the organic group time-averaged mirror symmetry. Thus, in the ^{1}H NMR spectrum the allylic portion of the {C_8H_{13}} ligand appears as a triplet of doublets at δ 4.43 due to the central methine hydrogen (H^2; J(HH) = 8, J(RhH) = 1 Hz) and a broad peak at δ 5.63 due to the two *syn*-CH protons (H^1 and H^3). Correspondingly the methine carbon atom (C^2) appears in the ^{13}C{^{1}H} NMR spectrum as a doublet at δ 99.4 (J(RhC) = 6 Hz), with the *syn* carbon atoms (C^1 and C^3) giving rise to a very broad peak around δ 93. The remaining CH_2 groups of the ring give rise to complex multiplets in the ^{1}H NMR spectrum in the range δ 2.47−1.35 (intensity ratio 2:2:2:1:1); the signal for the two hydrogens involved in the rapidly alternating C−H···Rh interactions is too broad to be seen. Likewise, the fluxional process causes all four of C^4, C^5, C^7, and C^8 to appear as a single very broad peak around δ 28.6 in the ^{13}C{^{1}H} NMR spectrum, with only C^6 sufficiently distant from Rh to be unaffected and hence seen as a much sharper singlet at δ 23.0.

Upon cooling, however, the "switching" of the C−H···Rh interaction between equivalent CH groups is slowed, and at 233 K it is arrested completely, at least on the NMR time scale. The {C_8H_{13}} ligand loses its apparent symmetry, and the proton involved in the agostic bond is seen as a broad resonance of unit relative intensity at δ −1.01 in the ^{1}H NMR spectrum, this relatively shielded chemical shift position being characteristic of the metal···H agostic interaction. Separate signals for all the other ^{1}H and ^{13}C nuclei in this ligand are also visible in their respective spectra and could be fully assigned by correlation spectroscopy (see Table 2).

An ^{11}B{^{1}H} NMR study on compound **7** showed five signals in the ratio 1:2:2:3:1 in the range δ 11.9 to −21.1, the overall shift to lower field (relative to compounds **2**−**6**; see Table 3) being consistent with the oxidation of the metal center. The spectrum at 233 K is almost identical to that at 293 K, except for some broadening at the lower temperature, as is to be expected. The observed pattern of ^{11}B resonances suggests the carborane fragment to retain time-averaged mirror symmetry

in solution, even upon cooling, an observation that is at odds with the variable-temperature ^1H and ^{13}C NMR data for the rhodium-bound $\{C_8H_{13}\}$ ligand. Although the reasons for this apparent discrepancy at present are not clear, it is conceivable that the loss of molecular symmetry seen at 233 K is simply not sufficient to separate individual ^{11}B resonances that are anyway rather broad and hence poorly resolved.

In contrast with the reaction between **1b** and the hydride-abstracting reagent $[Ph_3C][BF_4]$, treatment of a THF solution of **2** with the same reagent resulted in hydride abstraction at a cage {BH} vertex and then substitution of a THF molecule to form the zwitterionic compound [4-(cod)-7-$\{O(CH_2)_4\}$-*closo*-4,1,6-$RhC_2B_{10}H_{11}$] (**8**) in modest yields. The same reaction using $[NO][BF_4]$ as reagent gave similar results. Superior yields of **8** were achieved by introduction of CF_3SO_3Me to a solution of **2** in CH_2Cl_2/THF (5:1).

Compound **8** displays six resonances in its $^{11}B\{^1H\}$ NMR spectrum, having the intensity ratio 1:3(2 + 1 coincidence):2:1:2:1. The peak at lowest field, δ 20.9, remains a singlet in the fully proton-coupled ^{11}B spectrum, confirming loss of the terminal hydride from this boron vertex. The strong deshielding of this resonance suggested that a THF molecule had been substituted at this vertex, while the pattern of peak intensities indicated that C_s symmetry was retained in solution, and hence that the substitution has occurred on a boron vertex within the pseudo-mirror plane. A ^1H NMR study of **8** revealed resonances due to the cod ligand at δ 4.05 (a broad singlet due to the =CH groups) and 2.42 (a complex multiplet due to the CH_2 protons). In addition, the incorporation of a THF molecule was shown by a broad peak at δ 4.85 and a complex multiplet at δ 2.32, these two resonances being due to the α- and β-CH_2 protons (with respect to the oxygen atom), respectively.

An X-ray crystallographic study was undertaken upon a single crystal of **8** in order to identify the site of boron vertex substitution, and the resulting molecular structure is shown in Figure 7. The THF molecule is coordinated via the oxygen atom to B(7) (B(7)−O(71) = 1.5220(19) Å), donating a lone pair and rendering the $\{O(CH_2)_4\}$ moiety formally positively charged. The negative charge on the carborane ligand $\{C_2B_{10}H_{11}-O(CH_2)_4\}$ is thereby formally reduced by one. The integrity of the cod unit is maintained and the Rh center remains in the +1 oxidation state. Logically, it was anticipated that B(7) would be the site favored for substitution: the BH groups adjacent to the metal vertex would be expected to be the most hydridic—and therefore the most susceptible to hydride abstraction—and hence B(7), which is the more distant from the electronegative cage carbon atoms, is most likely to become substituted.

Consistent with this, we note that this {BH} unit is also very often involved in B−H→M interactions with *exo*-polyhedral M centers, for example, in compounds **3** and **6** above and in related $\{NiC_2B_{10}\}$ species.[6] Steric crowding and crystal packing must also be considered in the bimetallic complexes, and the precise electronic and geometric requirements for bonding the *exo*-polyhedral metal center must also be a factor. We believe that the structures ultimately adopted in the solid state result from a subtle interplay of all of these factors and will be better understood with the aid of detailed theoretical treatments. Qualitatively, however,

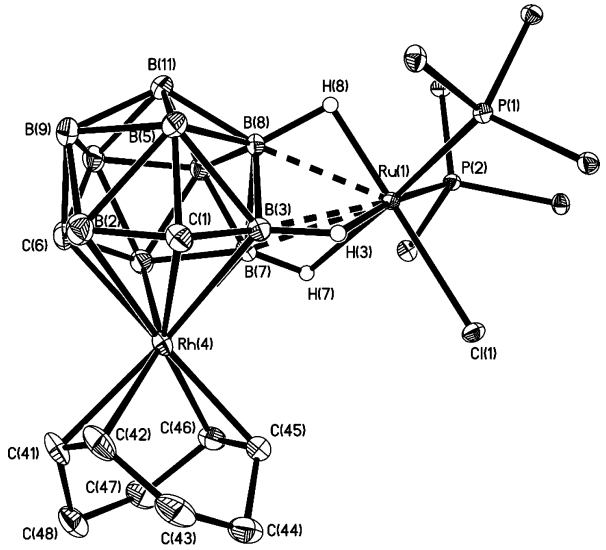

Figure 5. Structure of **6** showing the crystallographic labeling scheme. Selected bond lengths (Å) and angles (deg): Rh(4)−C(41) 2.212(2), Rh(4)−C(42) 2.203(2), Rh(4)−C(45) 2.158(2), Rh(4)−C(46) 2.144(2), C(41)−C(42) 1.396(3), C(45)−C(46) 1.407(3), B(3)···Ru(1) 2.324(2), B(7)···Ru(1) 2.465(2), B(8)···Ru(1) 2.261(2), Ru(1)−P(1) 2.2917(7), Ru(1)−P(2) 2.3390(7), Ru(1)−Cl(1) 2.3850(6); C(45)−Rh(4)−C(41) 87.63(9), C(46)−Rh(4)−C(41) 80.09(8), C(45)−Rh(4)−C(42) 79.87(9), C(46)−Rh(4)−C(42) 95.84(9), P(1)−Ru(1)−P(2) 101.64(2), P(1)−Ru(1)−Cl(1) 95.64(2), P(2)−Ru(1)−Cl(1) 88.99(2), P(1)−Ru(1)−B(3) 106.72(6), B(3)−Ru(1)−P(2) 147.47(5), B(3)−Ru(1)−Cl(1) 103.53(6), B(8)−Ru(1)−P(1) 108.89(6), B(8)−Ru(1)−P(2) 110.47(6), B(8)−Ru(1)−Cl(1) 144.00(6), P(1)−Ru(1)−B(7) 147.28(5), P(2)−Ru(1)−B(7) 104.45(5), Cl(1)−Ru(1)−B(7) 104.17(5).

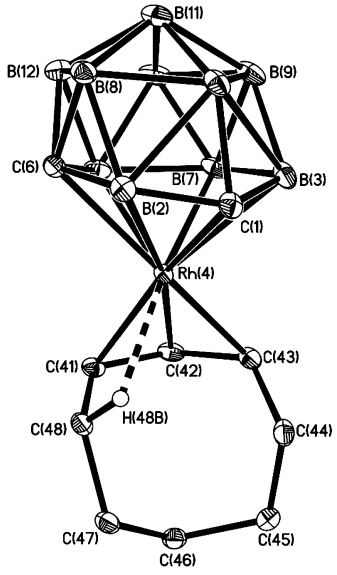

Figure 6. Structure of **7** showing the crystallographic labeling scheme. Selected bond lengths (Å) and angles (deg): Rh(4)−C(1) 2.1422(10), Rh(4)−B(2) 2.3010(12), Rh(4)−B(3) 2.3852(12), Rh(4)−C(6) 2.3567(11), Rh(4)−B(7) 2.1797(12), Rh(4)−B(10) 2.1887(13), Rh(4)−C(41) 2.1394(10), Rh(4)−C(42) 2.1279(10), Rh(4)−C(43) 2.1494(11), Rh(4)···C(48) 2.6052(11), Rh(4)···H(48B) 2.183(15), C(41)−C(42) 1.4067(15), C(42)−C(43) 1.4325(16); C(42)−Rh(4)−C(41) 38.49(4), C(42)−Rh(4)−C(43) 39.13(4), C(41)−Rh(4)−C(43) 70.45(4), C(41)−C(42)−C(43) 121.22(10).

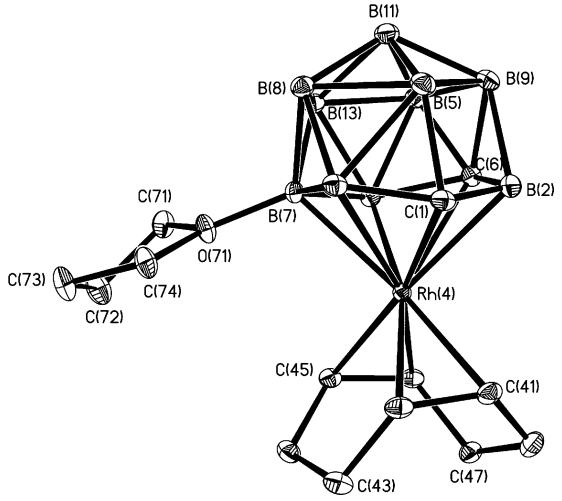

Figure 7. Structure of **8** showing the crystallographic labeling scheme. Selected bond lengths (Å) and angles (deg): Rh(4)−C(1) 2.1191(14), Rh(4)−B(2) 2.3296(18), Rh(4)−B(3) 2.3699(17), Rh(4)−C(6) 2.4571(15), Rh(4)−B(7) 2.2945(16), Rh(4)−B(10) 2.2532(18), Rh(4)−C(41) 2.1611(15), Rh(4)−C(42) 2.1523(15), Rh(4)−C(45) 2.1567(14), Rh(4)−C(46) 2.1599(14), C(41)−C(42) 1.408(2), C(45)−C(46) 1.407(2), B(7)−O(71) 1.5220(19); C(45)−Rh(4)−C(41) 96.35(6), C(46)−Rh(4)−C(41) 80.07(6), C(42)−Rh(4)−C(45) 80.65(6), C(42)−Rh(4)−C(46) 88.59(6), Rh(4)−B(7)−O(71) 115.37(10).

it seems clear that there may often be only small energetic differences between the various *exo*-polyhedral sites, as demonstrated by the solution fluxional behavior of many of these species.

Conclusion

We have synthesized compound **2**, containing the 13-vertex (cyclooctadiene)rhodacarborane monoanion [4-(cod)-*closo*-4,1,6-$RhC_2B_{10}H_{12}]^-$, and have investigated its reactions with electrophiles. Further examples of the rare class of bimetallic species that contain a 13-vertex metallacarborane are provided by the formation of **3**−**6**. In compound **3** a direct metal−metal bond exists between the *endo* rhodium and *exo* copper atoms and is supported by B−H⇀Cu agostic-type interactions from the carborane cage. In contrast, compounds **4**−**6** provide examples of bimetallic species in which no direct metal−metal connectivity exists, the *exo*-polyhedral metal fragment being bound to the periphery of the rhodacarborane solely by agostic interactions. Treatment of **3** with H^+ to give **7** has shown selectivity toward reaction with the cod ligand rather than the carborane cage, whereas the corresponding reaction with Me^+ has afforded **8** and potentially provides a general route to boron-substituted 13-vertex metallacarboranes.

Experimental Section

General Considerations. All reactions were carried out under an atmosphere of dry, oxygen-free nitrogen using Schlenk line techniques. Some subsequent manipulations were performed in the air, where indicated. Solvents were distilled from appropriate drying agents under nitrogen prior to use. Petroleum ether refers to that fraction of boiling point 40−60 °C. Chromatography columns (typically ca. 15 cm in length and ca. 2 cm in diameter) were packed with silica gel (Acros, 60−200 mesh). Filtrations through Celite typically employed a pad ca. 5 cm deep. NMR spectra were recorded at the following frequencies (MHz): ^{1}H, 360.1; ^{13}C, 90.6; ^{11}B, 115.5; ^{31}P, 145.8. The compounds $[Rh_2(\mu\text{-}Cl)_2(cod)_2]$,[11] $[CuCl(PPh_3)]_4$,[12] $[Rh(cod)(PPh_3)_2][PF_6]$,[13] and $[RuCl_2(PPh_3)_3]$[14] were obtained by literature methods; all other reagents were used as received.

Synthesis of $[N(PPh_3)_2][4\text{-}(cod)\text{-}closo\text{-}4,1,6\text{-}RhC_2B_{10}H_{12}]$. A THF (20 mL) solution of *closo*-1,2-$C_2B_{10}H_{12}$ (0.25 g, 1.73 mmol) was treated with Na cuttings (ca. 0.20 g, 8.70 mmol) and a catalytic amount of naphthalene, and the mixture stirred until a dark green coloration persists (ca. 20 min); the resulting solution of Na_2[*nido*-7,9-$C_2B_{10}H_{12}$] was used without isolation. Excess Na was removed using a spatula and $[Rh_2(\mu\text{-}Cl)_2(cod)_2]$ (0.42 g, 0.87 mmol) added and the resultant orange mixture stirred for 2 h. Solid $[N(PPh_3)_2]Cl$ (1.00 g, 1.73 mmol) was then added and the mixture stirred for 1 h, after which time volatiles were removed in vacuo, and the resulting residue was extracted with CH_2Cl_2 (30 mL). The extract was reduced in volume in vacuo to ca. 5 mL before being passed down a chromatography column using CH_2Cl_2/petroleum ether (2:1) as eluant to yield a single orange band, which was collected and reduced to dryness to yield $[N(PPh_3)_2][4\text{-}(cod)\text{-}closo\text{-}4,1,6\text{-}RhC_2B_{10}H_{12}]$ (**2**) (0.50 g) as a brown solid.

Synthesis of Bimetallic Compounds. (i) To a CH_2Cl_2 solution (10 mL) of **2** (0.150 g, 0.17 mmol) was added $[CuCl(PPh_3)]_4$ (0.061 g, 0.04 mmol) followed by $Tl[PF_6]$ (0.059 g, 0.17 mmol). After stirring for 4 h the mixture was filtered (Celite), and the filtrate concentrated and passed down a chromatography column using CH_2Cl_2/petroleum ether (1:1) as eluant to yield a single yellow band. This was collected and reduced to dryness, and the residue washed with petroleum ether (3 × 30 mL) to yield [4-(cod)-3,4,7-{$Cu(PPh_3)$}-3,7-(μ-H)$_2$-*closo*-4,1,6-$RhC_2B_{10}H_{10}$] (**3**) (0.055 g) as a yellow solid.

(ii) In the same way, a THF solution (15 mL) of **2** (0.150 g, 0.17 mmol), treated with $[Rh(cod)(PPh_3)_2][PF_6]$ (0.15 g, 0.17 mmol), yielded [4-(cod)-3,8-{$Rh(PPh_3)_2$}-3,8-(μ-H)$_2$-*closo*-4,1,6-$RhC_2B_{10}H_{10}$] (**4**) (0.10 g) as an orange microcrystalline solid.

(iii) Similarly, compound **2** (0.150 g, 0.17 mmol) in CH_2Cl_2 (10 mL) with $[Rh_2(\mu\text{-}Cl)_2(cod)_2]$ (0.041 g, 0.08 mmol) and $Tl[PF_6]$ (0.059 g, 0.17 mmol) gave [4-(cod)-3,8-{Rh(cod)}-3,8-(μ-H)$_2$-*closo*-4,1,6-$RhC_2B_{10}H_{10}$] (**5**) (0.047 g) as yellow microcrystals.

(iv) By an analogous procedure, a CH_2Cl_2 solution (15 mL) of **2** (0.150 g, 0.17 mmol) treated with $[RuCl_2(PPh_3)_3]$ (0.083 g, 0.17 mmol) yielded [4-(cod)-3,7,8-{$RuCl(PPh_3)_2$}-3,7,8-(μ-H)$_3$-*closo*-4,1,6-$RhC_2B_{10}H_9$] (**6**) (0.060 g) as a microcrystalline red solid.

Synthesis of $[4\text{-}(1\text{−}3\text{-}\eta^3\text{-}C_8H_{13})\text{-}closo\text{-}4,1,6\text{-}RhC_2B_{10}H_{12}]$. To a cooled (−50 °C) CH_2Cl_2 solution (10 mL) of **2** (0.150 g, 0.17 mmol) was added CF_3SO_3H (30 μL, 0.34 mmol), and the resulting mixture was stirred and allowed to warm to room temperature. After stirring for ca. 30 min, the mixture was evaporated to dryness and the residue passed down a chromatography column at 0 °C using CH_2Cl_2/petroleum ether (2:3) as eluant to yield a single orange band, which was collected and reduced to dryness. The residue was washed with petroleum ether (3 × 30 mL) and dried in vacuo, yielding [4-(1−3-

(10) (a) Speckman, D. M.; Knobler, C. B.; Hawthorne, M. F. *Organometallics* **1985**, *4*, 1692. (b) Salzer, A.; Buchmann, B.; Schmalle, H. *Acta Crystallogr.* **1991**, *C47*, 275. (c) Bortolin, M.; Bucher, U. E.; Ruegger, H.; Venanzi, L. M.; Albinati, A.; Lianza, F.; Trofimenko, S. *Organometallics* **1992**, *11*, 2514. (d) Vigalok, A.; Uzan, O.; Shimon, L. J. W.; Ben-David, Y.; Martin, J. M. L.; Milstein, D. *J. Am. Chem. Soc.* **1998**, *120*, 12539. (e) Trepanier, S.; Sterenberg, B. T.; McDonald, R.; Cowie, M. *J. Am. Chem. Soc.* **1999**, *121*, 2613. (f) Budzelaar, P. H. M.; Moonen, N. N. P.; de Gelder, R.; Smits, J. M. M.; Gal, A. W. *Eur. J. Inorg. Chem.* **2000**, 753. (g) Urtel, H.; Meier, C.; Eisentrager, F.; Rominger, F.; Joschek, J. P.; Hofmann, P. *Angew. Chem., Int. Ed.* **2001**, *40*, 781. Note that the hydrogen atom involved in such interactions is often not located crystallographically, and therefore reported distances may not be entirely reliable.

(11) Giordano, G.; Crabtree, R. H. *Inorg. Synth.* **1990**, *28*, 88.

(12) Jardine, F. H.; Rule, J.; Vohra, G. A. *J. Chem. Soc. A* **1970**, 238.

(13) Schrock, R. R.; Osborn, J. A. *J. Am. Chem. Soc.* **1971**, *93*, 2397.

(14) Hallman, P. S.; Stephenson, T. A.; Wilkinson, G. *Inorg. Synth.* **1970**, *12*, 237.

Table 4. Crystallographic Data for Compounds 2·0.5C_7H_8, 3, 4, 5, 6·2.5C_4H_8O, 7, and 8

	2·0.5C_7H_8	**3**	**4**	**5**	**6**·2.5C_4H_8O	**7**	**8**
formula	$C_{49.5}H_{58}B_{10}NP_2Rh$	$C_{28}H_{39}B_{10}CuPRh$	$C_{46}H_{54}B_{10}P_2Rh_2$	$C_{18}H_{36}B_{10}Rh_2$	$C_{56}H_{74}B_{10}ClO_{2.5}P_2RhRu$	$C_{10}H_{25}B_{10}Rh$	$C_{14}H_{31}B_{10}ORh$
fw	939.92	681.11	982.75	566.39	1196.62	356.31	426.40
space group	*C*2/*c*	$P2_1/n$	*Pbca*	$P2_1/n$	$P\bar{1}$	$P2_1/c$	$P2_1/c$
a, Å	39.741(3)	8.7860(10)	20.9484(11)	7.0539(17)	10.485(2)	11.5693(7)	13.443(3)
b, Å	10.3844(10)	14.2795(16)	19.8989(10)	29.096(7)	13.808(3)	9.3582(6)	7.9226(18)
c, Å	28.915(2)	24.498(2)	21.2596(11)	11.478(3)	21.618(5)	15.3295(10)	18.780(4)
α, deg					98.632(11)		
β, deg	128.431(4)	93.882(4)		105.456(9)	102.624(11)	105.326(3)	105.767(8)
γ, deg					109.847(10)		
V, Å^3	9347.8(14)	3066.5(6)	8862.1(8)	2270.6(10)	2785.6(11)	1600.67(18)	1925.0(7)
Z	8	4	8	4	2	4	4
ρ_{calcd}, g cm^{-3}	1.336	1.475	1.473	1.657	1.427	1.479	1.471
μ(Mo Kα), mm^{-1}	0.471	1.303	0.851	1.458	0.715	1.046	0.887
no. of reflns measd	49 074	41 943	78 856	11 747	92 494	26 706	25 030
no. of indept reflns	11 974	8040	16 683	4902	20 402	5815	5786
R_{int}	0.0644	0.0366	0.0501	0.1171	0.0659	0.0371	0.0389
wR2, R1[a] (all data)	0.1104, 0.0741	0.0681, 0.0338	0.0740, 0.0574	0.1514, 0.0936	0.0911, 0.0618	0.0564, 0.0248	0.0553, 0.0318
wR2, R1 (obs[b] data)	0.1002, 0.0438	0.0652, 0.0260	0.0682, 0.0323	0.0771, 0.0607	0.0858, 0.0377	0.0541, 0.0204	0.0531, 0.0227

[a] wR2 = $[\sum\{w(F_o^2 - F_c^2)^2\}/\sum w(F_o^2)^2]^{1/2}$; R1 = $\sum||F_o| - |F_c||/\sum|F_o|$. [b] $F_o > 4\sigma(F_o)$.

η^3-C_8H_{13})-*closo*-4,1,6-$RhC_2B_{10}H_{12}$] (**7**) (0.080 g) as an orange microcrystalline solid.

Synthesis of [4-(cod)-7-{$O(CH_2)_4$}-*closo*-4,1,6-$RhC_2B_{10}H_{11}$]. A solution of **2** (0.100 g, 0.11 mmol) in CH_2Cl_2/THF (5:1, 10 mL) was treated with CF_3SO_3Me (32 μL, 0.28 mmol). The resulting mixture was stirred for 3 h before being evaporated to dryness and the residue subjected to column chromatography using CH_2Cl_2/petroleum ether (2:3) as eluant. A single orange band was obtained, which was collected and reduced to dryness, and the residue washed with petroleum ether (3 × 30 mL) to yield [4-(cod)-7-{$O(CH_2)_4$}-*closo*-4,1,6-$RhC_2B_{10}H_{11}$] (**8**) (0.039 g) as an orange-yellow powder.

X-ray Crystallographic Structure Determinations. Diffraction quality crystals of compounds **2**−**4** and **6**−**8** were obtained by slow diffusion of petroleum ether into toluene/acetone (**2**), CH_2Cl_2 (**3**, **4**, **7**, **8**), or THF (**6**) solutions at −30 °C. This methodology was not possible for compound **5** due to its appreciable solubility in the precipitating solvent; hence, cooling of a saturated petroleum ether solution provided suitable crystals.

Experimental data for all determinationsare are presented in Table 4. X-ray intensity data were collected at 110(2) K on a Bruker-Nonius X8 APEX CCD area-detector diffractometer using Mo Kα X-radiation. Several sets of narrow data "frames" were collected at different values of θ, for various initial values of ϕ and ω, using 0.5° increments of ϕ or ω. The data frames were integrated using SAINT;[15] the substantial redundancy in data allowed an empirical absorption correction (SADABS)[15] to be applied, based on multiple measurements of equivalent reflections.

All structures were solved using conventional direct methods[15,16] and refined by full-matrix least-squares on all F^2 data using SHELXTL version 6.10 and SHELXL-97.[16] The locations of the cage-carbon atoms were verified by examination of the appropriate internuclear distances and the magnitudes of their isotropic thermal displacement parameters. All non-hydrogen atoms were assigned freely refining, anisotropic displacement parameters. An exception to this was the structure of **5**, for which the data were only of modest quality due to the availability of only small, platelike crystals that were rather poorly diffracting. In this case, a mixture of constraints and restraints were applied to the *exo* cod ligand, using the SIMU and EADP cards in SHELXL.[16]

All carborane H atoms, including those involved in B−H→M agostic-type interactions, were located in difference maps and were allowed free refinement of their positions; their thermal parameters were also freely refined, with the exception of the cage hydrogens in **5** and **6**, which were assigned fixed isotropic thermal parameters, calculated as $U_{iso}(H) = 1.2 \times U_{iso}$(parent). For compounds **2**−**6** and **8**, the hydrogen atoms in organic groups were included in calculated positions and allowed to ride on their parent atoms, with fixed isotropic thermal parameters, calculated as $U_{iso}(H) = 1.2 \times U_{iso}$(parent) or $U_{iso}(H) = 1.5 \times U_{iso}$(parent) for methyl hydrogens; for **7**, the H atoms of the organic moiety were refined without restraint.

Compound **2** cocrystallizes with one-half molecule of toluene per asymmetric unit, located on a C_2 axis (Wyckoff position *e*). This molecule was located such that there were two statistically equivalent positions for the methyl group; thus the three carbons of the phenyl ring were assigned unit occupancy, but that of the methyl group was fixed at one-half, as required by site symmetry. The solvate was otherwise treated as above and refined without difficulty.

Two-and-a-half molecules of THF cocrystallize per formula unit of compound **6**, of which the two whole solvate molecules are located in general space. One of these is ordered, but in the other one the β-CH_2 unit is disordered over two possible sites. Both such methylene groups were included with refining complementary occupancies, their ratio being approximately 48:52 at convergence. The half-molecule of THF solvate was located near an inversion center (Wyckoff position *c*) with, in effect, two alternative positions for the oxygen atom (each with half-occupancy) such that the overall arrangement of the six atom positions (4 × C, 2 × O) resembled the cyclohexane "chair" conformation. In reality, this situation also requires two alternative positions for each carbon atom, but these could not be resolved; the model instead simply had two carbon atoms with unit occupancy and one-half-occupancy oxygen atom (in the asymmetric unit) and was refined with some restraints (DFIX card in SHELXL[16]).

Acknowledgment. We thank the Robert A. Welch Foundation for support (Grant AA-1201). The Bruker-Nonius X8 APEX diffractometer was purchased with funds received from the National Science Foundation Major Research Instrumentation Program (Grant CHE-0321214).

Supporting Information Available: Full details of crystallographic analyses as a CIF file. This material is available free of charge via the Internet at http://pubs.acs.org.

OM049102E

(15) *APEX 2*, version 1.0-5; Bruker AXS: Madison, WI, 2003.
(16) *SHELXTL* version 6.10; Bruker AXS: Madison, WI, 2000.